PROCEEDINGS, 42nd Workshop on Geothermal Reservoir Engineering
Stanford University, Stanford, California, February 13-15, 2017
SGP-TR-212

Correlation between joint roughness anisotropy on deep cores and seismic propagation direction in Pohang EGS site, Korea

Melvin Diaz[1], Sehyeok Park[2], Sun Yeom[3], Kwang Yeom Kim[4], Ki-Bok Min[5]

[1]University of Science and Technology, 176 Gajeong-dong, Daejeon, 34113, Rep. of Korea

[2,5]Seoul National University, 1 Gwanak-ro, Gwanak-gu, Seoul 08826, Rep. of Korea

[3,4]Korea Inst. of Civil Eng. and Building Tech., 238 Goyangdae-Ro, Gyeonggi-Do, 10223, Rep. of Korea

[1]mdiaz@kict.re.kr, [2]sehyeok@snu.ac.kr, [3]duatjs@kict.re.kr, [4]kimky@kict.re.kr, [5]kbmin@snu.ac.kr

Keywords: Rock joint roughness, JRC, anisotropy, deep cores, hydraulic stimulation, shearing direction.

ABSTRACT

South Korea launched its first enhanced geothermal project in 2010 aiming to install MW class binary power plant. Until now, two wells have been drilled and a first hydraulic fracturing stimulation was conducted for 23 days in early 2016. The first well, PX-1, has a measured depth of 4,127 m, while the second well (PX-2), has reached a profundity of 4,348 m.

During the completion of PX-2, rock core samples were recovered at a depth of 4,219 m, and they comprise a length of 3.6 m with a diameter of 10 cm with open and closed joints crossing them. Using the X-ray computed tomography, the specimens were scanned to analyze internal features as well as to obtain 3D representations in order to compute physical properties. For this study, nine joint surfaces were extracted, with an approximate angle of 30 degrees in relation to the drilling direction. Among other parameters, the Joint Roughness Coefficient (JRC) was measured at different directions. Nearly all surfaces displayed roughness directionality indicating clear anisotropy in the joint roughness. The average orientation of the maximum JRC values is 161.7 degrees measured anticlockwise from the horizontal, and view from the footwall plane. Furthermore, the JRC directionality was compared with the seismicity propagation direction in the hydraulic stimulation of Pohang PX-2 well and the estimated shearing direction based on the back-estimation of in-situ stress orientation. The estimated shearing direction showed good correlations with the minimum JRC orientation and the seismicity propagation direction, which implies that the analysis with joint roughness directionality can serve as an indirect method to estimate the shearing directions and investigate the orientation of paleo-stress.

1. INTRODUCTION

Late on 2010, South Korea started its first enhanced geothermal project located in the eastern coastline, in the city of Pohang (Figure 1). The project incorporates different institutions with the target to install a MW binary plant (Song et al., 2015). Up to now, wells PX-1 and PX-2 have been completed, including a sidetrack to the first one. During the course of drilling well PX-2, rock core samples of 10 cm diameter were retrieved at 4,219 m, and they served to obtain physical and mechanical properties of the rock matrix. Furthermore, various joints cross the core specimens, and since they are of major importance due to their influence on the hydraulic and mechanical behavior of rock masses, we decided to carry out a detailed roughness characterization of these discontinuities. Joints commonly act as fluid channels, and they are also a source of major deformations (Wittke, 2014). Deep rock joints are crucial for petroleum and geothermal engineering because their roughness characteristics are important for coupled hydromechanical processes in terms of caprock leakage for CO2 geosequestration, and for permeability improvement of enhanced geothermal systems (EGS) (Rutqvist & Stephansson, 2003; Lewicki et al., 2007).

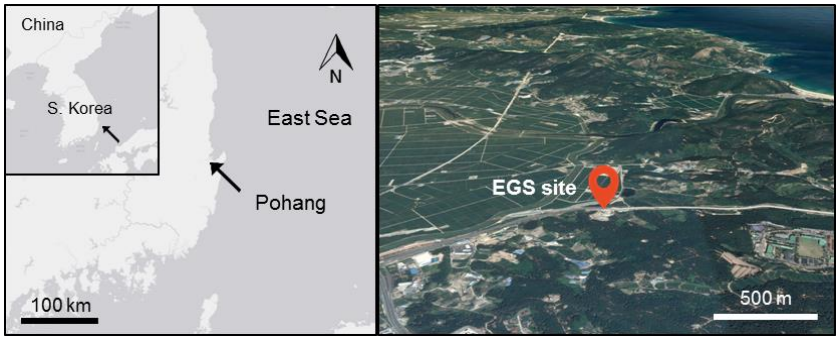

Figure 1: EGS pilot project, located in the coastal city of Pohang, Republic of Korea. The project started on 2010, and targets to install a MW power plant.

On the other hand, earthquakes data in major fault zone areas had been used to compute slip direction and rate (Molnar and Sykes, 1969). Recently, laboratory seismic data has also been used to monitor slip movement triggered by fluid injection into a natural fault (Guglielmi et al., 2015). Additionally, Yeo et al. (1998) conducted a series of laboratory experiments using radial and unidirectional flow, and concluded that the permeability increases in the direction perpendicular to the shearing orientation. Therefore, the estimation of the slip movement direction during hydraulic stimulation can add important information about the created fluid paths.

The current study focuses on the roughness characterization of rock joints from deep cores. An X-ray computer tomography (CT) scanner was employed to obtain detailed 3D models of each rock core. Joint roughness coefficient (JRC) was used to closely follow the anisotropic nature of the natural joint surfaces. Moreover, seismic data collected during the first hydraulic stimulation was employed to estimate the shearing direction during stimulation. This first stimulation took place early on 2016 and it lasted 23 consecutive days. Results from JRC measurements and shearing direction estimation are compared and discussed, and possible implications are presented.

2. ROUGHNESS MEASUREMENT ON JOINTS FROM DEEP CORES

2.1 Rock cores and joints

The rock samples were extracted at a depth of 4,219 m from well PX-2, and were disposed into core boxes to facilitate their transportation. The rock cores have a diameter of 10 cm, with varying length and size. Also, the core pieces were grouped into sections, as it is shown in Figure 2. Various joints cross the specimens, however, two main groups were identified. The first group of joints intersects the cores at around 25° in relation to the vertical or coring direction, while the second group of joints does it at around 80°. Because a major fault within the targeted reservoir area was defined with a 67° dip, and 25° dip direction, we decided to consider only the first group of joints assuming that they are subparallel to this major fault. Table 1 lists their individual angles in relation to the coring direction.

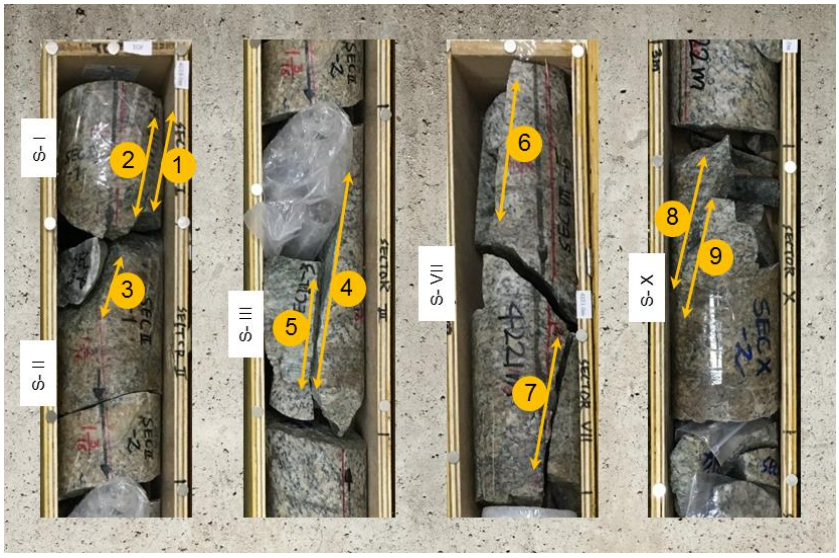

Figure 2: Deep rock cores with diameter of 10 cm extracted from well PX-2 at a depth of 4.22 km. The legends "s - " denote the section the sample belongs to, while the circle digits indicate the rock joints considered in this study. These joints cross the rock cores at around 25° in relation to the coring orientation.

2.2 Joint surface acquisition and JRC measurement

Joint surface data was acquired though the industrial X-ray computer tomography (CT) facility at the Korea Institute of Civil Engineering and Building Technology (KICT). The advantage of this technology over conventional laser scanner is that it enables the possibility of inspecting internal as well as external features of an object based on 3D rendered models. The selected scanning conditions and point cloud data resolution are the same as used by Diaz et al. (2017). The temperature and humidity were set as 21° Celsius, and 31% respectively, while the voltage and current were adjusted at 240 kVp, and 500 mA. The time of exposure was 1 s, with 1800 number of projections. The source object distance, as well as the pixel pitch were adjusted to each core piece in order to maximize the quality of the CT images. On the other hand, the point cloud data resolution was fixed at 0.1 mm.

VG studio MAX, a specialized software for the analysis and interpretation of CT data was used for joint surface selection and 3D point cloud data generation. Figure 3 shows color contour maps of the nine joint surfaces plotted at the same scale to help appreciate the differences in sizes and shapes. The joints are drawn relative to a local coordinate system placed on the foot wall of the joint. Three pairs of joints (1, 2; 4, 5; and 8, 9) are coplanar, although the duplet formed by joints 4 and 5 varies in size.

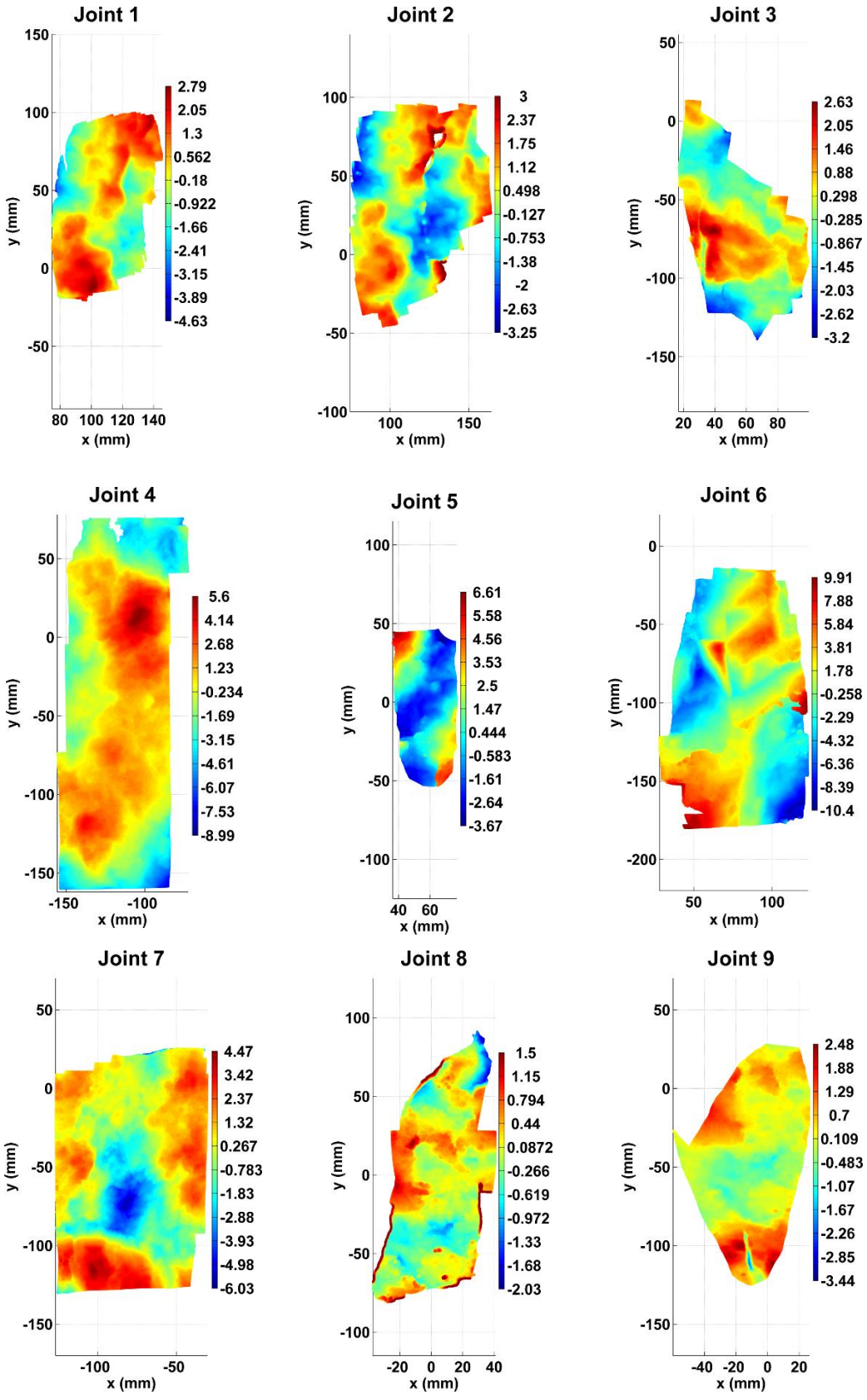

Figure 3: Color contour maps of nine deep rock joints. The joint surfaces are plotted at the same scale and drawn relative to a local coordinate system that was placed on the foot wall of each joint.

2.3 Measured JRC anisotropy

The chosen parameter for the surface roughness characterization of these rock joints was the Joint Roughness Coefficient (JRC) because of its wide usage. This parameter was first proposed by Barton and Choubey (1977), and it was originally estimated by visual comparison of a particular rock joint profile with 10 typical cross sections of defined JRC. Later, Tse and Cruden (1979) proposed two mathematical relations for the calculation of JRC, and introduced the root mean square of the first deviation of the profile and the structure function as the main variables for these equations. Later, Yu and Vayssade (1991) pointed out the changing value of Z_2 due to different sampling intervals. Thereafter, various equations have been proposed for JRC estimation (Li and Zhang, 2015). As a way to avoid sampling distance issues, we selected equation E7 proposed by the former mentioned authors which is a recalculation of Barton and de Quadros (1997) equation, and it is derived from 112 digitized rock profiles. The equation is expressed as follows.

$$JRC = 158.7575 \times \left(\frac{R_z}{L} \right) + 3.9076 \tag{1}$$

where R_Z and L are maximum height of the profile and the length, respectively.

Because this equation computes JRC along cross sections, we implemented an algorithm to measure multiple profiles as a way to obtain average values along different orientations. Figure 4 (a) illustrates the angular separation of these orientations, while (b) shows the process of cross section generation along one orientation based on 3D point cloud data. The point sampling distance along each profile or cross section was set to 0.4 mm, and the distance between profiles was 2.5 mm. This process was repeated every 5° to closely follow the anisotropic surface of these deep rock joints.

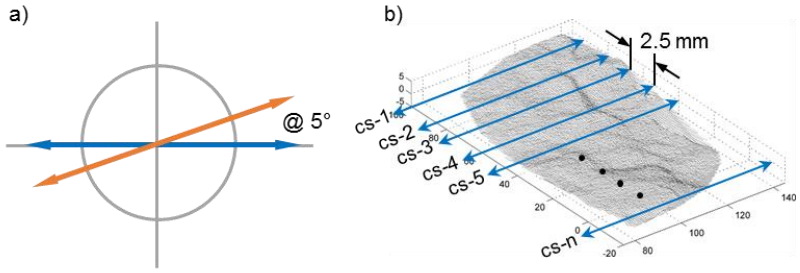

Figure 4: Process of JRC measurement on each joint surface; a) angular separation of 5° between different orientations to estimate JRC anisotropy, and b) generation of multiple cross sections along a particular orientation.

The final JRC value per orientation was estimated as the average of the values located one standard deviation above and under the mean value as a way to consider only those representative values.

2.4 JRC measurement results

A summary of geometric characteristics of these joint surfaces is listed in Table 1. The angle measured in relation to the coring direction was obtained after fitting a plane through the cloud data that represents each surface. The area, maximum peak, lowest valley, and maximum height are also provided as general descriptors of these rock surfaces. The maximum height is simply the vertical distance between the maximum peak and lowest valley.

Table 1: Joint geometric parameters.

Joint	Angle* (degrees)	Area (cm^2)	Maximum peak (mm)	Lowest valley (mm)	Maximum height (mm)
1	18.4°	68.6	2.8	-4.5	7.3
2	18.8°	99.4	3.0	-3.2	6.2
3	22.8°	79.6	2.6	-3.2	5.8
4	9.2°	174.5	5.7	-9.2	14.9
5	8.5°	35.2	6.6	-3.6	10.2
6	12.7°	131.9	9.4	-10.7	20.2
7	6.2°	139.6	4.5	-6.0	10.5
8	22.9°	94.4	1.7	-2.0	3.7
9	25.5°	86.0	2.5	-3.4	5.9

*measured relative to the vertical or coring direction.

The average angle of these joints in relation to the coring direction is 16.1°, which is equivalent to a 73.8° dip angle. In terms of the superficial area, joint 4 has the highest extension with 174.5 cm^2 while joint 5 is the smallest with an area of 35.2 cm^2. The largest maximum height is found in joint 6, a joint that is also among the largest in area.

Moreover, the JRC measurements are presented in Figure 5 and drawn in polar plots, where the averaged JRC values per orientation are plotted every 5°. Most surfaces are clearly anisotropic in terms of JRC, with values ranging from 5 up to 20. However, joints 3, 7, and 9 display lower degree of anisotropy. To aid determining the degree of anisotropy, we fitted ellipses to the measured JRC points and computed the ratio of maximum to minimum values. Joints, 1, 2, 4, 5, 6, and 8 gave ratios of 1.45, 1.44, 1.54, 1.58, 1.34, and 1.43 respectively. On the other hand, joints 3, 7, and 9 showed lower values of 1.14, 1.18 and 1.07 respectively. Furthermore, the ellipse fitting process helped also to trace the orientation of the maximum JRC value. Besides joint 3, all the other joints yield a similar orientation with an average angle of 161.6°. All these angles were measured starting from the positive x-axis in a counter-clockwise manner on their local coordinate system, placed on the foot wall face of each joint.

Joints 1 and 2 are coplanar and have similar JRC values as well as the joint area and the degree of anisotropy. In contrast, joint 3 that is located immediately bellow them has different maximum JRC value with different orientation. However, it is important to notice that its maximum value is nearly the same as in joints 1 and 2 along that orientation, suggesting that the superficial features captured within its area need to be complemented. Joints 4 and 5 are also coplanar, but differ in size. However, their values and orientation of maximum JRC are alike. Joints 6 and 7 are also anisotropic, but appear to have small secondary maximum values with different orientations. Joint 8, although is not the smallest in area, has the lowest JRC values and yet is still anisotropic with a ratio of 1.43. Finally joint 9 appears to be more isotropic than the rest.

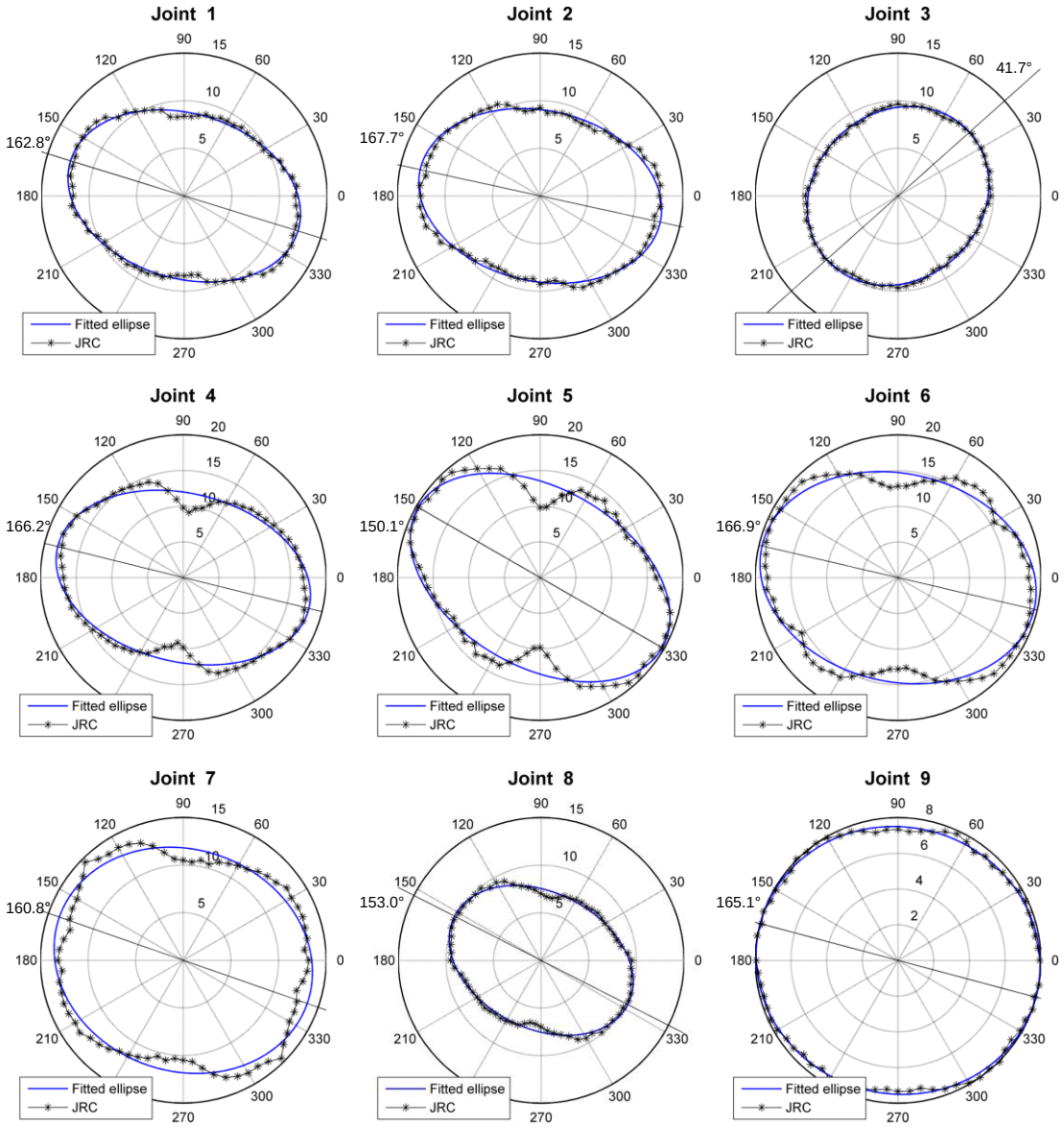

Figure 5: JRC values measured every 5° starting from the positive x-axis in a counter-clockwise manner on their local coordinate system that was set on the foot wall of each joint. The fitted ellipse served to calculate the anisotropy ratio, as well as the orientation of the maximum value.

3. COMPARISONS WITH SHEARING DIRECTION

The second part of this study covers the comparisons of joint roughness directionality with the estimated shearing direction on a fault plane and the propagation direction of seismic cloud observed from the hydraulic stimulation of PX-2 well.

3.1 Propagation direction of the seismic cloud

Induced seismic events had been captured and located during the first hydraulic stimulation at the PX-2 well of Pohang EGS site. Plan views of the seismic cloud are shown in Figure 6 with time order from February 2nd to 24th, 2016. It is noticeable that the seismic event started at January 29th propagated to south-west direction as the stimulation had been continued to February 24th. Overall trend of the propagation direction was approximated as the red arrow shown in Figure 6 by fitting a straight line crossing the first event occurred at January 29th using least squares method. The azimuth of propagation direction in plan view was determined as 252.3°.

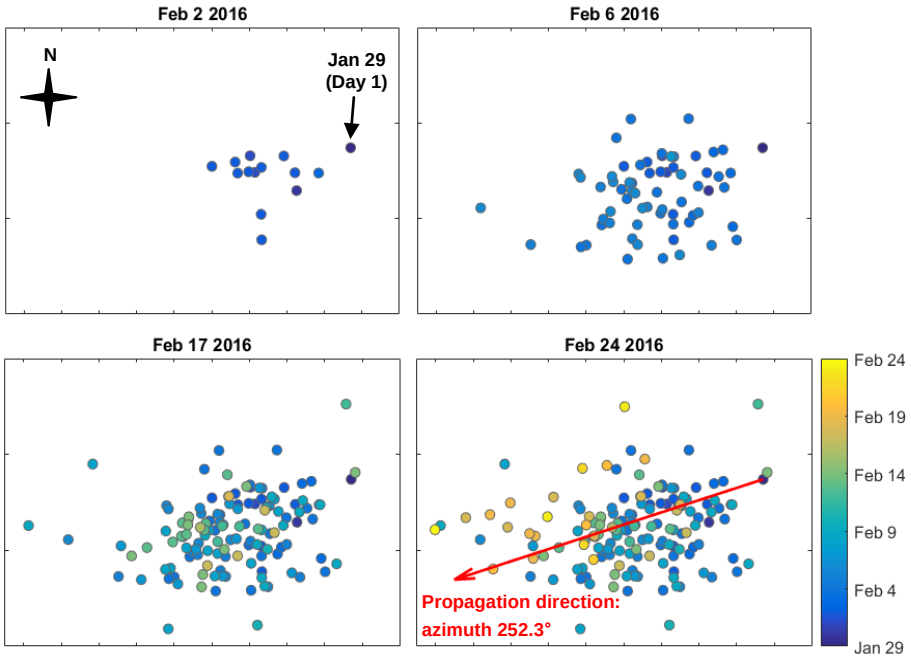

Figure 6: Plan views of the seismic cloud observed from the hydraulic stimulation of Pohang PX-2 well, showing the propagation of seismic events in time order

3.2 Estimation of the shearing direction on a fault plane

When the effect of the roughness anisotropy on the mechanical behavior of a target fracture is assumed to be negligible, it is possible to estimate the direction of shear slip movement on that fracture plane using the information of in-situ stress condition and fracture plane orientation.

Assuming that vertical stress is one of the principal stress, the in-situ principal stress tensor in principal direction can be expressed as

$$\tau^{pri} = \begin{bmatrix} S_{H\max} & 0 & 0 \\ 0 & S_{h\min} & 0 \\ 0 & 0 & S_V \end{bmatrix}, \tag{2}$$

where $S_{H\max}$ is the maximum horizontal stress, $S_{h\min}$ is the minimum horizontal stress, and S_V is the vertical stress.

When the in-situ stress tensor is rotated to the axes on which +x is east and +y is north, it is expressed as

$$\tau^{o} = L\tau^{pri}L^{T}, \quad L = \begin{bmatrix} \cos(\theta-\pi/2) & \sin(\theta-\pi/2) & 0 \\ -\sin(\theta-\pi/2) & \cos(\theta-\pi/2) & 0 \\ 0 & 0 & 1 \end{bmatrix}, \tag{3}$$

where τ^{o} is the rotated in-situ stress tensor and θ is the azimuth of $S_{H\max}$ measured clockwise from north.

Based on Eq. (2), the traction vector and resolved normal and shear stresses on a fracture plane can be calculated using the fracture plane normal n, as follows:

$$\begin{cases} p(n) = \tau^o n \\ \sigma_n = (p \cdot n)n \\ \tau_n = p - \sigma_n \end{cases} \quad (4)$$

where $p(n)$ is the traction vector on a fracture, σ_n is the resolved normal stress and τ_n is the resolved shear stress. The direction of shear slip movement on a target fracture plane can be estimated as the direction of τ_n.

Using Eq. (2) ~ (4), the first-order estimation of shearing direction on the target fault in Pohang reservoir was conducted based on the orientation of the major fault of 67° dip and 25° dip direction and the in-situ stress model suggested by Kim et al (2016). The in-situ stress model was suggested based on the hydraulic fracturing test, borehole breakout and drilling-induced tensile fracture observations in 670~810 m depth of Pohang EXP-1 well located 3.8 km from PX-2 well. The in-situ stress condition for shearing direction estimation was prepared by extrapolating the stress model of EXP-1 to the target depth of 4.3 km, as shown in Table 2. In-situ stress condition estimated from Pohang CO_2 geo-sequestration test site, which is located 8.8 km and 7.5 km from PX-2 well and EXP-1 well, respectively, also suggested consistent results for the stress ratio, the azimuth of maximum horizontal stress, and the stress regime (Chang et al., 2016).

The results in Figure 7 shows the first-order estimation of shearing direction as blue line on the fault plane. Additionally, the direction perpendicular to shearing is shown as red line on the fault plane. However, the azimuth of shearing direction on a plan view in Figure 7 (a) was estimated as 280.3°, which has considerable discrepancy with the observed shearing propagation direction indicated as the red arrow in Figure 6.

Table 2: in-situ stress model of Pohang reservoir used for the first-order estimation of shearing direction

Depth	Vertical stress (S_V)	Max. horizontal stress ($S_{H\max}$)	Min. horizontal stress ($S_{h\min}$)	$S_{H\max}$ azimuth	Stress ratio ($S_{H\max}/S_{h\min}$)	Stress regime
4,278 m	110.25 MPa	138.8 MPa	81.7 MPa	130°	1.7	Strike-slip faulting

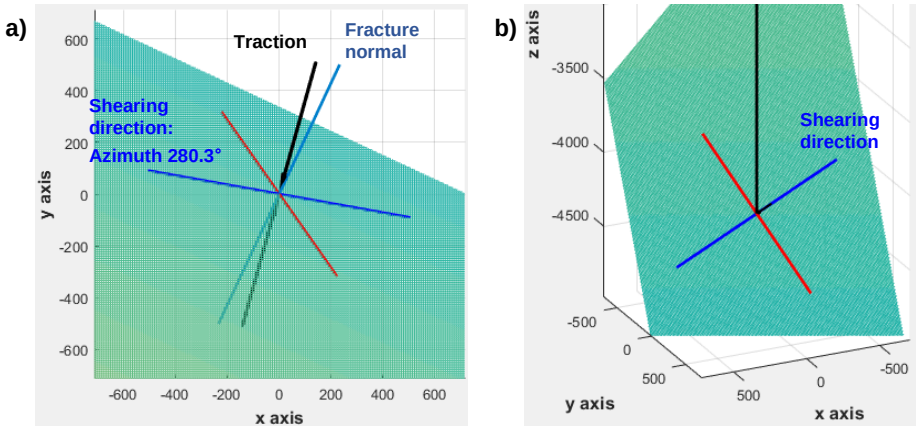

Figure 7: Result of the first-order estimation of shearing direction shown as blue line on a fault plane – a) plan view from +z direction; b) view from the upper fracture normal direction

One of the interpretation on the cause of this discrepancy between the observed propagation of seismic cloud and the estimated shearing direction can be suggested as the rotation of in-situ stress direction. Considering that the depth ranges of 4.3 km deep reservoir and the shallow formations within 1 km depth, the stress rotation could possibly occur within this section. Based on the same fault plane orientation and Eq. (2) ~ (4), the back-estimation of in-situ stress orientation was conducted by matching the resulted direction of shearing with the observed propagation direction of seismic cloud shown in Figure 6, while the in-situ stress magnitudes were maintained as Table 2. As the result, the azimuth of maximum horizontal stress was determined as 119.7° when the resulted shearing direction was estimated as Figure 8.

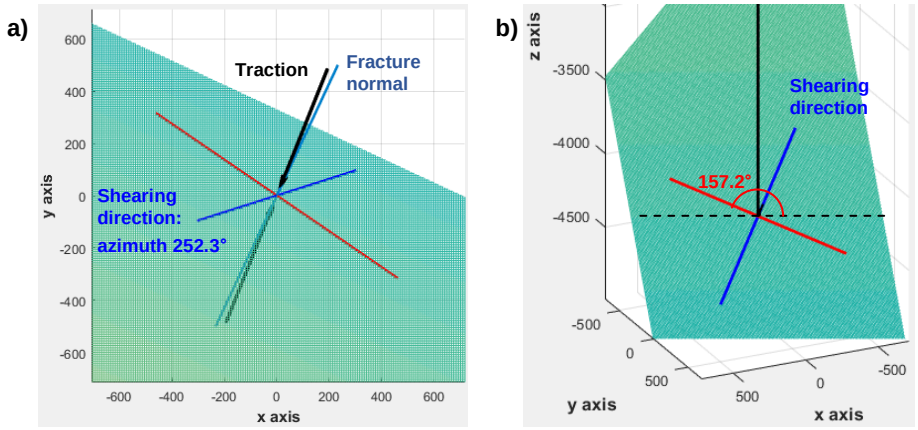

Figure 8: estimation of shearing directions resulted from the back-estimation of in-situ stress orientation – a) plan view from +z direction; b) view from the upper fracture normal direction

Comparing Figure 6 and Figure 8, one can easily notice that the estimated shearing direction in Figure 8 (a) is exactly matched with the seismicity propagation direction in Figure 6, which was done by back-estimation of in-situ stress orientation. More interest can be put onto the comparison of Figure 5 and Figure 8 (b); after matching the shearing direction to the seismicity propagation direction, the red line in Figure 8, which is perpendicular to the shearing direction on the fault plane, is very closely oriented with the average orientation of maximum JRC in Figure 5. Recalling the angle for maximum JRC orientation in Figure 5 is 161.6°, the angle for the orientation perpendicular to the estimated shearing direction in Figure 8 (b) is 157.2°, showing only 4.4° difference.

In other words, it can be argued that the estimated shearing direction on the fault plane, matched with the seismicity propagation direction, was closely oriented with the minimum JRC direction obtained from the cored joints that is expected to be sub-parallel to the target fault. The implication of this result can be stated as one of the followings: 1) the paleo-stress at 4.3 km depth of Pohang reservoir that resulted the current joint roughness anisotropy is similar with the current stress state, thus the seismicity propagation in the hydraulic stimulation of PX-2 occurred along the direction similar to the minimum JRC orientation; or 2) shearing propagation in the stimulation of PX-2 well was considerably affected by the JRC anisotropy, in case it is not negligible.

4. CONCLUSIONS

A correlation between joint roughness on deep rock cores and shearing direction during hydraulic stimulation of Pohang EGS was carried out. The first part focused on the roughness characterization of the rock joints, and a total of 9 joints were selected for this purpose. Data acquisition of the joint surfaces was done by scanning the rock cores with an X-ray CT equipment, and 3D cloud data files were generated for each targeted joint. To account for the anisotropic nature of joints, the cloud data files served to compute average JRCs of multiple profiles along different orientations separated every 5°.

The measured JRC values ranged from 6.6 up to 19.6, and nearly all surfaces display a defined anisotropy. Ellipses were fitted to estimate the anisotropic JRC ratio, and also to identify the orientation of the maximum values. Almost all maximum values fallen into a similar orientation, and their average angle was estimated as 161.6° when measured from the positive x-axis in a counter-clockwise manner of a coordinate system placed on the foot wall.

Backward determination of the maximum horizontal stress azimuth was conducted by matching the estimated shearing direction with the seismicity propagation direction, which resulted the azimuth of 119.7°. The resulted direction of shearing estimation showed a good correlation with the minimum JRC direction of the 73.8° dip fracture planes, assuming they are sub-parallel to the 67° dip angle and 25° dip direction of the major fault within the targeted reservoir.

This correlation implies that surface roughness anisotropy can serve as an indirect method to estimate shearing directions, and that the paleostress that generated the major fault in Pohang reservoir was very close to the current in-situ stresses.

ACKNOWLEDGEMENTS

This work was carried out in the framework of the European Union's Horizon 2020 research and innovation programme, DESTRESS(No 691728) and funded by the international R&D programme (No. N0002098) of Korea Institute for Advancement of Technology (KIAT).

REFERENCES

Barton, N., and Choubey, V.: The shear strength of rock joints in theory and practice, *Rock Mechanics*, 10(1-2), (1977), 1-54.

Chang, C., Jo, Y., Quach, N., Shinn, Y.J., Song, I., Kwon, Y.K.: Geomechanical Characterization for the CO2 Injection Test Site, Offshore Pohang Basin, SE Korea, *Proceedings*, 50th US Rock Mechanics/Geomechanics Symposium, Houston, Texas, June, 2016.

Diaz, M.B., Kim, K.Y., Yeom, S., Park, S., Zhuang, L., Min, K.B.: Surface Roughness Characterization of Open and Closed Joints in Deep Cores using X-ray Computed Tomography. *Manuscript submitted for publicatio*n, (2017).

DeMets, C.: A new estimate for present-day Cocos-Caribbean plate motion: Implications for slip along the Central American volcanic arc. *Geophysical Research Letters*, 28(21), (2001), 4043-4046.

Guglielmi, Y., Cappa, F., Avouac, J.P., Henry, P. and Elsworth, D.: Seismicity triggered by fluid injection–induced aseismic slip. *Science*, 348(6240), (2015), 1224-1226.

Kim, H., Min, K-B., Bae, S.H., Stephansson, O.: Integrated in-situ stress estimation by hydraulic fracturing and borehole observation at EXP-1 hole in Pohang of Korea, *Proceedings*, 7th Rock Stress Symposium, Tampere, Finland, 2016, 333-340

Lewicki, J.L., Birkholzer, J. and Tsang, C.F.: Natural and industrial analogues for leakage of CO2 from storage reservoirs: identification of features, events, and processes and lessons learned. *Environmental Geology*, 52(3), (2007), 457.

Li, Y., and Zhang, Y.: Quantitative Estimation of Joint Roughness Coefficient Using Statistical Parameters, *International Journal of Rock Mechanics and Mining Sciences*, 77, (2015), 27-35.

Molnar, P. and Sykes, L.R.: Tectonics of the Caribbean and Middle America regions from focal mechanisms and seismicity. *Geological Society of America Bulletin*, 80(9), (1969), 1639-1684.

Rutqvist, J. and Stephansson, O.: The role of hydromechanical coupling in fractured rock engineering. *Hydrogeology Journal*, 11(1), (2003), 7-40.

Song, Y., Lee, T.J., Jeon, J., and Yoon, W.S.: Backgroud and Progress of the Korean EGS Pilot Project, *Proceedings*, World Geothermal Congress, Melbourne, Australia, 2015, 19-25 April.

Tse, R., and Cruden, DM.: Estimating joint roughness coefficients. *Int J Rock Mech Min Sci Geomech Abstr*.16(5), 1979, 303-307.

Wittke, W.: Rock Mechanics Based on an Anisotropic Jointed Rock Model (AJRM). *Ernst & Sohn;* 2014.

Yeo, I.W., De Freitas, M.H. and Zimmerman, R.W.: Effect of shear displacement on the aperture and permeability of a rock fracture. *International Journal of Rock Mechanics and Mining Sciences*, 35(8), (1998), 1051-1070.

Yu, X., and Vayssade, B.: Joint Profiles and Their Roughness Parameters, *International journal of rock mechanics and mining sciences & geomechanics abstracts*, *Pergamon*, 28.4, (1991), 333-336.